Talanta 83 (2010) 682–685

Contents lists available at ScienceDirect

Talanta

journal homepage: www.elsevier.com/locate/talanta

Short communication

Effect of phase stability degradation of bismuth on sensor characteristics of nano-bismuth fixed electrode

Gyoung-Ja Lee, Chang Kyu Kim, Min Ku Lee*, Chang Kyu Rhee

Nuclear Materials Research Division, Korea Atomic Energy Research Institute (KAERI), Daedeok-Daero 1045 (150, Deokjin-dong), Yuseong-gu, Daejeon, 305-353, Republic of Korea

ARTICLE INFO

Article history:
Received 20 July 2010
Received in revised form 1 October 2010
Accepted 1 October 2010
Available online 8 October 2010

Keywords:
Nano-bismuth fixed electrode
Phase stability degradation
Square-wave anodic stripping voltammetry
Reproducibility
Sensitivity

ABSTRACT

Effect of phase stability degradation of bismuth on sensor characteristics of nano-bismuth fixed electrode has been investigated using square-wave anodic stripping voltammetry technique, scanning electron microscopy (SEM) and X-ray diffraction (XRD) spectroscopy. From the analyses of square-wave anodic stripping voltammograms (SWASV) repetitively measured on the nano-bismuth fixed electrode, it was found that the oxidation peak currents dropped by 81%, 68% and 59% for zinc, cadmium and lead, respectively, after the 100th measurement (about 400 min of operation time). The sphere bismuth nanoparticles gradually changed to the agglomerates with petal shape as the operation time increased. From the analyses of SEM images and XRD patterns, it is confirmed that the oxidation of Bi into $BiOCl/Bi_2O_2CO_3$ and the agglomeration of bismuth nanoparticles caused by the phase change decrease a reproducibility of the stripping voltammetric response. Moreover, most of the bismuth becomes BiOCl at pH 3.0 and bismuth hydroxide, $Bi(OH)_3$ at pH 7.0, which results in a significant decrease in sensitivity of the nano-bismuth fixed electrode.

1. Introduction

Since the suggestion of bismuth as a substitute for mercury electrode in electrochemical stripping analysis of trace heavy metals, there have been extensive studies on development of environmentally-friendly voltammetric sensors based on bismuth electrodes. Recently, the decade of electroanalysis with bismuth-based electrodes was reviewed [1] to celebrate many scientific activities and achievements for the past 10 years from the publication of the first pioneering report [2]. In our previous works [3–7], it has been reported that nano-bismuth fixed electrode with a larger surface area exhibits a higher sensitivity comparing to the bismuth film electrode. Furthermore, time-consuming procedures consisting of pre-plating and polishing steps can be avoided by using nano-bismuth fixed electrode. The attractive and promising nano-bismuth fixed electrode makes it possible to apply the electrode to an automatic on-line system as well as on-site portable system for a trace metal analysis.

It has been well known that the voltammetric response of the bismuth electrode is greatly influenced by various experimental variables such as pH of electrolyte solution [3,8–11], square-wave voltammetry parameters (pulse height, pulse width and step height) [3,7,11,12], deposition time/potential [3,4,6,7,9–16] and adsorption of surface-active compounds [12,17,18], etc. The microstructure of bismuth-based electrode also affects the sensor characteristics. For bismuth film electrode, the microscopic studies have been extensively carried out using optical microscopy (OM) [19], scanning electron microscopy (SEM) [2,15,20–26], scanning electrochemical microscopy (SECM) [27], atomic force microscopy (AFM) [28–30] and X-ray diffraction (XRD) method [31]. The surface morphology, density, uniformity and thickness of bismuth film were investigated with the changes of plating potential/time, composition of the plating solution and other experimental conditions for the preparation of bismuth film.

On the other hand, there are relatively few literatures [32–34] dealing with the microscopic study for the nano-bismuth electrode. In particular, an in-depth study on sensor characteristics of nano-bismuth electrode considering phase stability as well as surface morphology has not been carefully investigated. In this respect, the present work is aimed at exploring the effect of phase stability degradation of bismuth on sensor characteristics of the nano-bismuth fixed electrode by using square-wave anodic stripping voltammetry technique, SEM and XRD method. The changes in reproducibility of the nano-bismuth fixed electrode with operation time and in sensitivity of that electrode with solution pH were successfully explained by bismuth phase transition.

2. Experimental details

Bismuth nanopowders were synthesized by gas condensation (GC) method [35,36] using a micron powder feeding system, and then the prepared bismuth nanopowders were strongly fixed on

* Corresponding author. Tel.: +82 42 868 8565; fax: +82 42 868 4847.
E-mail address: leeminku@kaeri.re.kr (M.K. Lee).

0039-9140/$ – see front matter © 2010 Elsevier B.V. All rights reserved.
doi:10.1016/j.talanta.2010.10.007

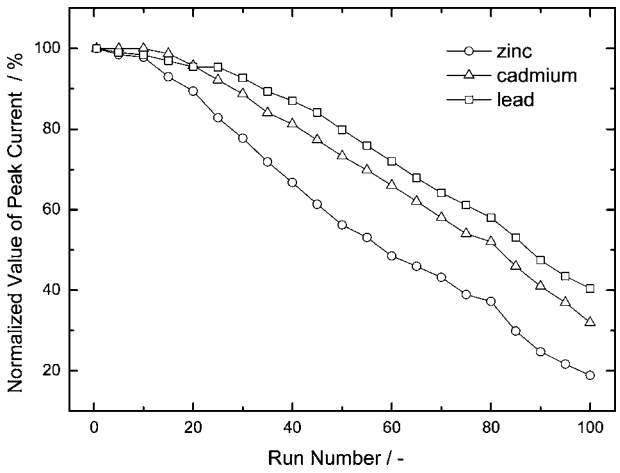

Fig. 1. Normalized oxidation peak currents of zinc, cadmium and lead which were obtained from the repetitively measured square-wave anodic stripping voltammograms (SWASV) for nano-bismuth fixed electrode in a solution containing 100 ppb zinc(II), cadmium(II), and lead(II) ions. Conditions: supporting electrolyte, 0.1 M NaAc and 0.025 M HCl solution (pH 5.0); working area, 0.1 cm^2; pulse height, 50 mV; pulse width, 10 ms; step height, 2.0 mV; deposition for 3 min at −1.35 V; cleaning at −0.4 V for 20 s.

the screen printed carbon electrode using Nafion solution. The detailed procedure of the preparation of nano-bismuth fixed electrode was described in our previous works [3–7]. A three-electrode electrochemical cell was employed for the anodic stripping voltammetry measurement. The nano-bismuth fixed electrode was used as a working electrode (active area = 0.1 cm^2). A platinum wire and a saturated calomel electrode (SCE) were used as the counter electrode and reference electrode, respectively. The supporting electrolyte was a 0.1 M NaAc and 0.025 M HCl solution of pH 5.0. The standard solutions of zinc(II), cadmium(II), and lead(II) ($\rho(Zn^{2+})$ = 1 g/l, $\rho(Cd^{2+})$ = 1 g/l, and $\rho(Pb^{2+})$ = 1 g/l) were purchased from AccuStandard, Inc., USA. The SWASV measurements were performed using potentiostat/galvanostat (Bistat, Princeton).

For the measurement of SWASV, the accumulation step of zinc, cadmium and lead proceeded for 3 min at −1.35 V under a magnetic stirring. Stirring was then stopped and after 10 s the SWASV was recorded in the potential range of −1.35 V to −0.4 V (vs. SCE) with a scan rate of 100 mV s^{-1} (pulse height: 50 mV, pulse width: 10 ms and step height: 2 mV). A prolonged series of 200 repetitive measurements of SWASV was performed for demonstrating the reproducibility of the nano-bismuth fixed electrodes. The cleaning step (20 s at −0.4 V) was employed between successive measurements. The SWASV was measured as a function of solution pH by controlling pH with HCl and NaOH addition.

The surface morphology of the nano-bismuth fixed electrode was observed by SEM with an accelerating voltage of 20 kV. The phase change of bismuth was studied by XRD with Cu K_α radiation (λ = 1.5406 Å) using the dried bismuth nanopowder after soaking in electrolyte solution for the same operation time of stripping voltammetry. A quantitative analysis of each phase from XRD profile-fitted peaks was conducted by using Jade 9.0 XRD software.

3. Results and discussion

Fig. 1 shows the normalized oxidation peak currents of zinc, cadmium and lead which were obtained from the repetitively measured SWASV for the nano-bismuth fixed electrode in a solution containing 100 ppb zinc(II), cadmium(II), and lead(II) ions. It can be seen from Fig. 1 that the oxidation peak currents gradually decreased with increasing run number and dropped by 81%, 68% and 59% drop for zinc, cadmium and lead, respectively, after

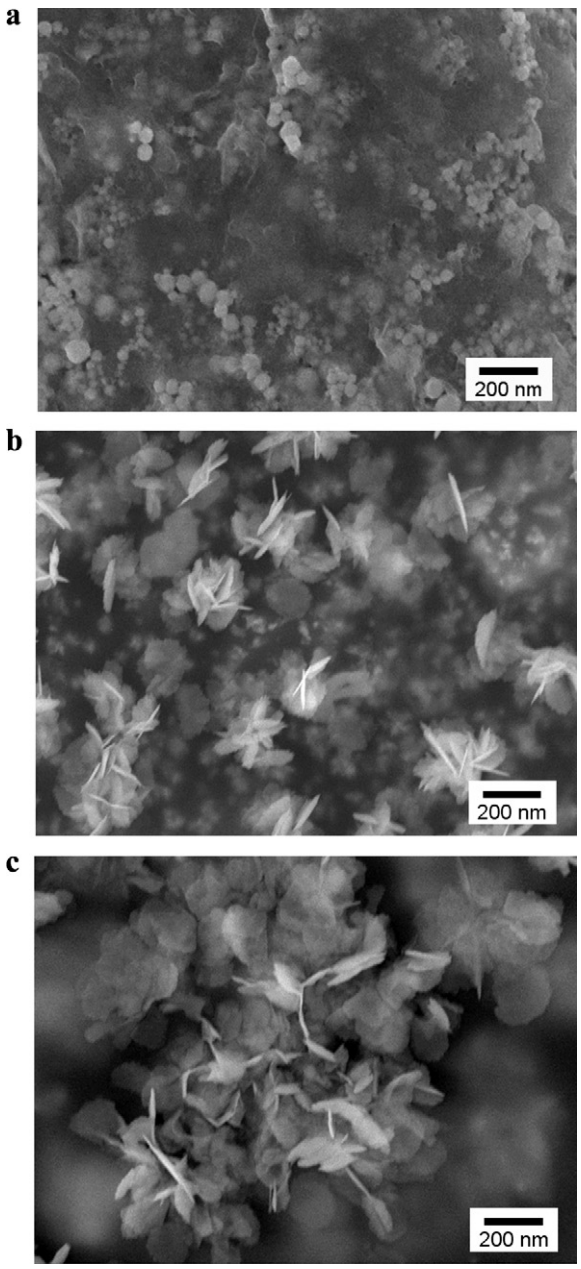

Fig. 2. Scanning electron microscopy (SEM) images of the nano-bismuth fixed electrode surfaces (a) as-prepared, (b) after the 50th (200 min of operation time) and (c) after the 100th (400 min of operation time) measurements of SWASV.

the 100th measurement (about 400 min of operation time). The decrease in oxidation peak current was high in the order of zinc, cadmium and lead. After the repetitive measurement of SWASV, a change in surface morphology of the sensor electrode was observed by SEM.

Fig. 2(a) illustrates the SEM image of the as-prepared nano-bismuth fixed electrode surface. It is noted from Fig. 2(a) that the spherical bismuth nanoparticles are well-connected with each other, using Nafion which is shown like cloud. Fig. 2(b) and (c) exhibits the SEM image of the sensor electrode after the 50th and 100th measurement of SWASV, respectively. As the repetitive measurements of SWASV proceeds, the sphere shape of bismuth nanoparticles was slowly transformed into the petal shape. After the 100th measurement of SWASV, most of sphere bismuth nanoparticles changed to the agglomerates with petal shape. Here, it should be emphasized that after soaking the nano-bismuth fixed

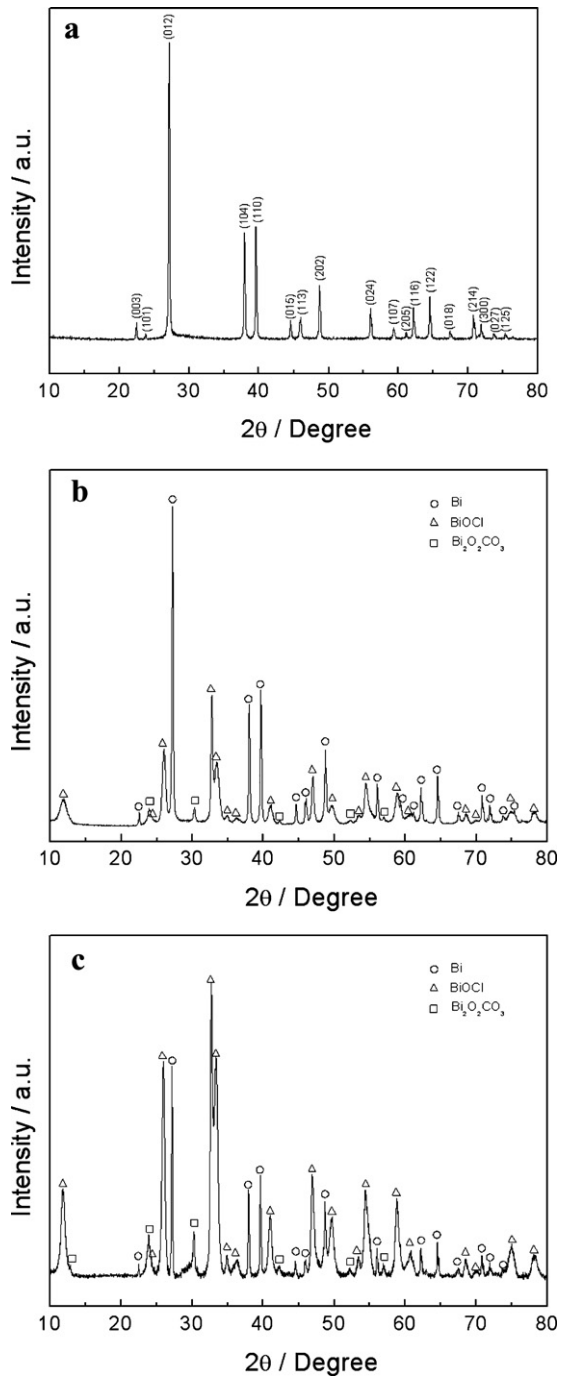

Fig. 3. X-ray diffraction (XRD) patterns obtained from the bismuth nanopowders (a) as-prepared and dried after soaking in electrolyte solution for (b) 200 min and (c) 400 min.

electrode in electrolyte solution without potential sweeping for the same operation time of stripping voltammetry, the electrode exhibited the same surfaces as Fig. 2(b) and (c). This strongly implies that the shape change of bismuth nanoparticles is caused by chemical reaction of bismuth with ions in electrolyte solution, not electrochemical reaction during potential sweeping.

It is shown in Fig. 3(a) that the XRD pattern of as-prepared bismuth nanoparticles reveals intense peaks which can be indexed as a rhombohedral structure of bismuth (Bi, JCPDS card No. 5-519). No other diffraction peaks corresponding to an oxide or an impurity were observed from the XRD pattern. This indicates that the resulting nanopowder synthesized by GC method is highly crystallized bismuth with a high purity. Fig. 3(b) and (c) demonstrates the XRD patterns obtained from the bismuth nanopowders after soaking in electrolyte solution for 200 min and 400 min as the same operation time of stripping voltammetry respectively. The XRD patterns exhibit the intense peaks which are indexed as bismuth (Bi, JCPDS card No. 5-519), tetragonal structure of bismuth oxychloride (BiOCl, JCPDS card No. 6-249) and tetragonal structure of bismuth oxycarbonate ($Bi_2O_2CO_3$, JCPDS card No. 41-1488).

From the quantitative analyses of the XRD patterns, the relative amounts of Bi, BiOCl and $Bi_2O_2CO_3$ after 200 min soaking were estimated to be 50.5 wt%, 30.2 wt% and 19.3 wt%, respectively. After 400 min soaking, the relative amounts of Bi, BiOCl and $Bi_2O_2CO_3$ were determined to be 7.3 wt%, 46.0 wt% and 46.7 wt%, respectively. As the soaking time of bismuth nanopowders in electrolyte solution increases, the relative amount of Bi decreases, but the relative amounts of BiOCl and $Bi_2O_2CO_3$ increase in value. Therefore, it is reasonable to think that the agglomerates with petal shape in Fig. 2(b) and (c) are BiOCl and $Bi_2O_2CO_3$. The oxidation of Bi into BiOCl/$Bi_2O_2CO_3$ and the agglomeration of bismuth nanoparticles caused by the phase change decrease a reproducibility of the stripping voltammetric response.

On the other hand, the change in sensitivity of the nano-bismuth fixed electrode as a function of solution pH can be clearly explained by the bismuth phase change. From the investigation of the pH effect on the SWASV over the pH range of 3.0–7.0, the optimum value of solution pH was determined to be 5.0 for the maximized voltammetric responses of zinc, cadmium and lead (not shown). If the acidity was higher or lower than the optimum value above, the voltammetric responses of zinc, cadmium and lead decreased. In particular, the oxidation peak currents of zinc, cadmium and lead almost disappeared at pH 3.0 and 7.0. A similar optimal pH range from 4.5 to 5.5 for the highest peak currents was also reported in the literature [8,10,11]. From the analyses of the XRD patterns, it was found that the bismuth had a strong oxidation in BiOCl form at pH 3.0 and hydrolysis in bismuth hydroxide, $Bi(OH)_3$ (JCPDS card No. 1-898) at pH 7.0. Thus, it is suggested that the solution pH significantly influences the phase stability of bismuth and the phase transition of pure bismuth to the other forms leads to a considerable decrease in sensitivity of the nano-bismuth fixed electrode.

4. Conclusion

From the analyses of successively measured SWASV, SEM images and XRD patterns, it is indicated that the oxidation of Bi into BiOCl/$Bi_2O_2CO_3$ and the agglomeration of bismuth nanoparticles caused by the phase change decrease a reproducibility of the stripping voltammetric response. In addition, most of the bismuth becomes BiOCl at pH 3.0 and $Bi(OH)_3$ at pH 7.0, which leads to a significant decrease in sensitivity of the nano-bismuth fixed electrode. From the above results, it is concluded that the phase stability of bismuth is closely related to the sensitivity as well as the reproducibility of the nano-bismuth fixed electrode, and hence the phase stability of bismuth should be considered as one of the important factors for the maximized electrochemical performance of the sensor electrode.

Acknowledgment

This work was supported by the Korea Atomic Energy Research Institute (KAERI) Project, Republic of Korea.

References

[1] I. Švancara, C. Prior, S.B. Hoćevar, J. Wang, Electroanalysis 22 (2010) 1405–1420.
[2] J. Wang, J. Lu, S.B. Hocevar, P.A.M. Farias, Anal. Chem. 72 (2000) 3218–3222.
[3] G.-J. Lee, H.M. Lee, C.K. Rhee, Electrochem. Commun. 9 (2007) 2514–2518.

[4] G.-J. Lee, H.M. Lee, Y.R. Uhm, M.K. Lee, C.K. Rhee, Electrochem. Commun. 10 (2008) 1920–1923.
[5] H.M. Lee, G.-J. Lee, H.J. Kim, Y.R. Uhm, H.J. Kim, M.K. Lee, C.K. Rhee, J. Nanosci. Nanotechnol. 10 (2010) 309–313.
[6] G.-J. Lee, C.K. Kim, M.K. Lee, C.K. Rhee, Electroanalysis 22 (2010) 530–535.
[7] G.-J. Lee, C.K. Kim, M.K. Lee, C.K. Rhee, J. Electrochem. Soc. 157 (7) (2010) J241–J244.
[8] S.B. Hocevar, B. Ogorevc, J. Wang, B. Pihlar, Electroanalysis 14 (2002) 1707–1712.
[9] C.E. Banks, J. Kruusma, R.R. Moore, P. Tomčík, J. Peters, J. Davis, Š. Komorsky-Lovrič, R.G. Compton, Talanta 65 (2005) 423–429.
[10] J. Wang, D. Lu, S. Thongngamdee, Y. Lin, O.A. Sadik, Talanta 69 (2006) 914–917.
[11] W.W. Zhu, N.B. Li, H.Q. Luo, Anal. Lett. 39 (2006) 2273–2284.
[12] G. Kefala, A. Economou, A. Voulgaropoulos, M. Sofoniou, Talanta 61 (2003) 603–610.
[13] J. Wang, J. Lu, S.B. Hocevar, B. Ogorevc, Electroanalysis 13 (2001) 13–16.
[14] S.B. Hocevar, J. Wang, R.P. Deo, B. Ogorevc, Electroanalysis 14 (2002) 112–115.
[15] G. Kefala, A. Economou, A. Voulgaropoulos, Analyst 129 (2004) 1082–1090.
[16] J. Kruusma, C.E. Banks, R.G. Compton, Anal. Bioanal. Chem. 379 (2004) 700–706.
[17] J. Wang, R.P. Deo, S. Thongngamdee, B. Ogorevc, Electroanalysis 13 (2001) 1153–1156.
[18] S. Legeai, O. Vittori, Anal. Chim. Acta 560 (2006) 184–190.
[19] C. Kokkinos, A. Economou, I. Raptis, C.E. Efstathiou, Electrochim. Acta 53 (2008) 5294–5299.
[20] E.A. Hutton, S.B. Hočevar, B. Ogorevc, Anal. Chim. Acta 537 (2005) 285–292.
[21] I. Svancara, L. Baldrianova, M. Vlcek, R. Metelka, K. Vytras, Electroanalysis 17 (2005) 120–126.
[22] L. Baldrianova, I. Svancara, M. Vlcek, A. Economou, S. Sotiropoulos, Electrochim. Acta 52 (2006) 481–490.
[23] V. Guzsvány, M. Kádár, F. Gaál, L. Bjelica, K. Tóth, Electroanalysis 18 (2006) 1363–1371.
[24] L. Cao, J. Jia, Z. Wang, Electrochim. Acta 53 (2008) 2177–2182.
[25] L.M.S. Nunes, R.C. Faria, Electroanalysis 20 (2008) 2259–2263.
[26] G. Grincienė, A. Selskienė, R. Verbickas, E. Norkus, R. Pauliukaite, Electroanalysis 21 (2009) 1743–1749.
[27] S.B. Hočevar, S. Daniele, C. Bragato, B. Ogorevc, Electrochim. Acta 53 (2007) 555–560.
[28] G.U. Flechsig, M. Kienbaum, P. Gründler, Electrochem. Commun. 7 (2005) 1091–1097.
[29] A. Królicka, A. Bobrowski, A. Kowal, Electroanalysis 18 (2006) 1649–1657.
[30] C. Kokkinos, A. Economou, M. Koupparis, Talanta 77 (2009) 1137–1142.
[31] C. Kokkinos, A. Economou, I. Raptis, C.E. Efstathiou, T. Speliotis, Electrochem. Commun. 9 (2007) 2795–2800.
[32] W. Zhang, H. Tang, P. Geng, Q. Wang, L. Jin, Z. Wu, Elecrtrochem. Commun. 9 (2007) 833–838.
[33] K.E. Toghill, G.G. Wildgoose, A. Moshar, C. Mulcahy, R.G. Compton, Electroanalysis 20 (2008) 1731–1737.
[34] X. Chen, S. Chen, W. Huang, J. Zheng, Z. Li, Electrochim. Acta 54 (2009) 7370–7373.
[35] B.S. Han, C.K. Rhee, M.K. Lee, Y.R. Uhm, IEEE Trans. Magnetics 42 (2006) 3779–3781.
[36] Y.R. Uhm, B.S. Han, M.K. Lee, S.J. Hong, C.K. Rhee, Mater. Sci. and Eng. A 449–451 (2007) 813–816.